MEASUEMENT OF OPTICS ERRORS AND SPACE CHARGE EFFECTS

K. Ohmi, Y. Sato, J. Takano, KEK, Tsukuba, Ibaraki, Japan
S. Hatakeyama, JAEA, Tokai, Ibaraki, Japan

Abstract

Emittance growth and beam loss due to the space charge force are enhanced by errors of the lattice. Nonlinearities of the space charge force and lattice components are integrated with Twiss and x-y coupling parameters into one turn map. Twiss and x-y coupling parameters are measureable quantities. We study space charge effects based on the measured Twiss-coupling parameters.

INTRODUCTION

Emittance growth and beam loss are caused by chaotic behavior near nonlinear resonances induced by space charge force and nonlinear accelerator components. One turn map including the space charge and the nonlinear components characterizes the nonlinear property for long term behavior. The space charge force is incorporated into one turn map by integrating with a finite propagation step. The one turn map is constructed by connecting the nonlinear transfer maps, the nonlinear accelerator components and space charge force, with linear transformation (represented by transfer matrix) between them.

The beam shape, which characterizes the space charge force, is determined by one turn map. The one turn map is determined self-consistently by the space charge map with the beam shape.

The linear optics parameters are measurable, where they are for zero intensity. Transfer matrix and revolution matrix is reconstructed by the measured optics parameters. One turn map is constructed with the measured optics parameters. The one turn map based on measured optics is deviated from the design one. Simulation using the map gives worse emittance growth and beam loss than design one. The degradation should appear in actual accelerators. The beam loss caused by the optics errors can be recovered by an optics correction.

In this paper, we discuss measurement of linear optics parameters. One turn map is constructed by the measured linear optics parameters, where the strength of nonlinear components is assumed to be correct. Simulations using the one turn map have been performed for J-PARC MR. Some results, which is preliminary at present, are shown.

LATTICE TRANSFORMATION AND SPACE CHARGE FORCE

One turn map ($\mathcal{M}$) is defined how dynamical variables, $\boldsymbol{x}(s) = (x, p_x, y, p_y, z, \delta)^t$, are tarnsferred in a revolution,

$$\boldsymbol{x}(s + C) = \mathcal{M}(s)\boldsymbol{x}(s), \qquad (1)$$

where C is the circumference. The transverse momentum is normalized by design momentum p_0, and the longitudinal variables are defined by arrival time and momentum deviation as $z = v(t_0 - t)$ $\delta = \Delta p/p_0$, respectively. One turn map including the space charge force is expressed as follows,

$$\mathcal{M}(s) = \prod_{i=0}^{N-1} \mathcal{M}_0(s_{i+1}, s_i)e^{-:\Phi(s_i):}, \qquad (2)$$

where $\mathcal{M}(s_{i+1}, s_i)$ is nonlinear transformation from s_i to s_{i+1}. $\Phi(s_i)$, which is the space charge potential, is given by solving Poisson equation with the beam distribution at s_i.

The expression using the symbol $:\Phi:$ is

$$e^{-:\Phi(s_i):}p_\ell = p_\ell - \frac{\partial\Phi(s_i)}{\partial x_\ell}. \qquad (3)$$

where $p_\ell = p_x, p_y$ or δ, and $x_\ell = x, y$ or z. The integration step ($\Delta s = s_{i+1} - s_i$) should be chosen $\Delta s \ll \beta$, since betatron phase advance for Δs should be small ($\ll 1$).

One turn map including only lattice nonlinear components is decomposed by nonlinear map of the components and transfer matrix between the components as follows,

$$\mathcal{M}_0(s) = \prod_{i=0}^{N_{nl}-1} M_0^{-1}(s_{i+1}, s_i)e^{-:H_{nl}(s_i):}. \qquad (4)$$

where $M(s_{i+1}, s_i)$ is transfer matrix from s_i to s_{i+1}, and

$$e^{-:H_{nl}(s_i):}p_\ell = p_\ell - \frac{\partial H_{nl}(s_i)}{\partial x_\ell}. \qquad (5)$$

For example, H_{nl} for sextupole magnet is expressed by

$$H_{nl}(s_i) = \frac{K_2(s_i)}{6}(x^3 - 3xy^2) \qquad K_2 = \frac{eB"}{p_0} \qquad (6)$$

One turn map including space charge force (Eq. 2) is expressed by the nonlinear transformation and linear transfer matrix as follows,

$$\mathcal{M}(s) = \prod_{i=0}^{N-1} M_0(s_{i+1}, s_i)e^{-:H_I(s_i):}, \qquad (7)$$

where $N = N_{nl} + N_{sc}$, and $H_I = \Phi$ or H_{nl}. Simulation codes for space charge effects have been developed based on the description in Eq. 7 [1].

ISBN 978-3-95450-118-2

LINEAR DYNAMICS AND MEASUREMENT OF LINEAR OPTICS PARAMETERS

One turn map for linear dynamics is represented by the 6×6 revolution matrix,

$$\boldsymbol{x}(s+C) = M_0(s)\boldsymbol{x}(s) \tag{8}$$

The revolution matrix is diagonalized blockwisely using a matrix (V) as follows, [2]

$$V(s)M_0(s)V(s)^{-1} = \begin{pmatrix} U_X & 0 & 0 \\ 0 & U_Y & 0 \\ 0 & 0 & U_Z \end{pmatrix} \equiv U \tag{9}$$

where 2×2 matrix is expressed by

$$U_i \equiv \begin{pmatrix} \cos\mu_i & \sin\mu_i \\ -\sin\mu_i & \cos\mu_i \end{pmatrix} \tag{10}$$

U represents rotation of phase space of three decoupled normalized variables

$$\boldsymbol{X}(s) = V(s)\boldsymbol{x}(s) \qquad \boldsymbol{X}(s+C) = U\boldsymbol{X}(s) \tag{11}$$

The phase rotation angle per revolution is $\mu_i = 2\pi\nu_i$, where ν_i is tune of each decoupled space X, Y, Z.

V is given by eigenvector of M [2]. V is parametrized by three matrices as follows,

$$V(s) = B(s)R(s)H(s) \tag{12}$$

Each matrix is expressed as follows,

$$B = \begin{pmatrix} B_X & 0 & 0 \\ 0 & B_Y & 0 \\ 0 & 0 & B_Z \end{pmatrix} B_i = \begin{pmatrix} \frac{1}{\sqrt{\beta_i}} & 0 \\ \frac{\alpha_x}{\sqrt{\beta_i}} & \sqrt{\beta_i} \end{pmatrix}, \tag{13}$$

$$R = \begin{pmatrix} r_0 & 0 & -r_4 & r_2 & 0 & 0 \\ 0 & r_0 & r_3 & -r_1 & 0 & 0 \\ r_1 & r_2 & r_0 & 0 & 0 & 0 \\ r_3 & r_4 & 0 & r_0 & 0 & 0 \\ 0 & 0 & 0 & 0 & 1 & 0 \\ 0 & 0 & 0 & 0 & 0 & 1 \end{pmatrix} \tag{14}$$

$$r_0 = \sqrt{1 - r_1 r_4 + r_2 r_3}$$

$$H = \begin{pmatrix} 1 & 0 & 0 & 0 & 0 & -\eta_x \\ 0 & 1 & 0 & 0 & 0 & -\eta'_x \\ 0 & 0 & 1 & 0 & 0 & -\eta_y \\ 0 & 0 & 0 & 1 & 0 & -\eta'_y \\ \eta'_x & -\eta_x & \eta'_y & \eta_y & 1 & 0 \\ 0 & 0 & 0 & 0 & 0 & 1 \end{pmatrix} \tag{15}$$

H decomposed M into 4×4 and 2×2 matrices, HMH^{-1}. This operation is extraction of betatron coordinates subtracting dispersion. R decomposes HMH^{-1} into three 2×2 matrices with well-known form as

$$M_i(s) = \begin{pmatrix} \cos\mu_i + \alpha_i \sin\mu_i & \beta_i \sin\mu_i \\ -\gamma_i \sin\mu_i & \cos\mu_i - \alpha_i \sin\mu_i \end{pmatrix}. \tag{16}$$

B normalizes the betatron motion from elliptic to circular trajectory in the decoupled phase space.

Parameters containing in B (α_i and β_i) are Twiss parameters. Other parameters in R and H can be regarded as a kind of Twiss parameters. We call them extended Twiss parameters in this paper.

Betatron motion is treated by introducing the betatron coordinates, which are extracted by H. Experimentally betatron motion is extracted by a transverse kick at dispersion free section. In this case, it is sufficient to take into account the matrix M with 4×4, and dynamical variable is $\boldsymbol{x}_\beta = (x, p_x, y, p_y)_\beta = \boldsymbol{x} - \boldsymbol{\eta}$.

Courant-Snyder invariant is expressed by [3]

$$W_{X,Y} = 2J_{X,Y} = \boldsymbol{x}_\beta^T A^R_{X,Y} \boldsymbol{x}_\beta, \tag{17}$$

where

$$A^R_i \equiv RS_4 A_i R^{-1} \qquad i = X, Y. \tag{18}$$

$A_{X,Y}$ is written by Twiss parameters as follows,

$$A_X = \left(\begin{array}{cc|c} \gamma_X & \alpha_X & 0 \\ \alpha_X & \beta_X & \\ \hline \multicolumn{2}{c|}{0} & 0 \end{array}\right) \tag{19}$$

and

$$A_Y = \left(\begin{array}{c|cc} 0 & \multicolumn{2}{c}{0} \\ \hline 0 & \gamma_Y & \alpha_Y \\ & \alpha_Y & \beta_Y \end{array}\right). \tag{20}$$

The matrix S is the symplectic metric,

$$S_4 = \begin{pmatrix} S_2 & 0 \\ 0 & S_2 \end{pmatrix} \qquad S_2 = \begin{pmatrix} 0 & 1 \\ -1 & 0 \end{pmatrix}. \tag{21}$$

MEASUREMENT OF EXTENDED TWISS PARAMETERS

Extended Twiss parameters are measured using turn-by-turn monitors at J-PARC MR. Injection error for x or y direction at dispersion free section applied, approximately X or Y mode is induced, respectively.

The betatron trajectory of X mode with W_X is expressed by an ellipse in 4 dimensional phase space as follows,

$$\delta(\boldsymbol{x}^T A^R_X \boldsymbol{x} - W_X) \tag{22}$$

The trajectory contains $y-p_y$ component in proportional to the coupling strength. Figure 1 shows an example of phase space trajectory given by a measurement.

Extended Twiss parameters are determined by the second order moment in the phase space trajectory [4]. The second order moment of the betatron trajectory is given by,

$$J_X \begin{pmatrix} r_0^2\beta_X & -r_0^2\alpha_X & r_0(-\beta_X r_1 + \alpha_X r_2) & r_0(-\beta_X r_3 + \alpha_X r_4) \\ & r_0^2\gamma_X & r_0(\alpha_X r_1 - \gamma_X r_2) & r_0(\alpha_X r_3 - \gamma_X r_4) \\ & & \beta_X r_1^2 - 2\alpha_X r_1 r_2 + \gamma_X r_2^2 & \beta_X r_1 r_3 - \alpha_X(r_1 r_4 + r_2 r_3) + \gamma_X r_2 r_4 \\ & & & \beta_X r_3^2 - 2\alpha_X r_3 r_4 + \gamma_X r_4^2 \end{pmatrix} \tag{23}$$

ISBN 978-3-95450-118-2

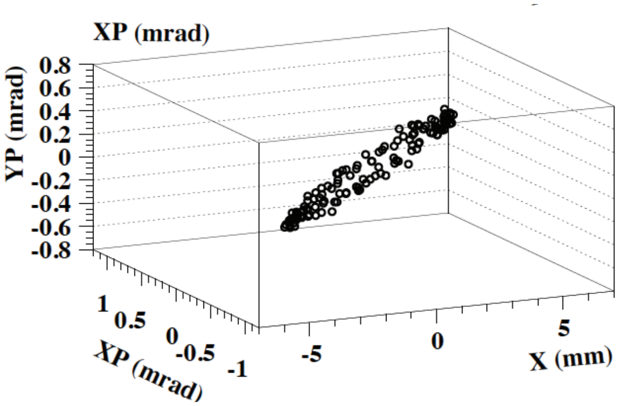

Figure 1: Phase space trajectory in $x-p_x-p_y$ phase space.

$$J_Y \begin{pmatrix} \beta_Y r_4^2 + 2\alpha_Y r_2 r_4 + \gamma_Y r_2^2 \\ \beta_Y r_3 r_4 + \alpha_Y (r_1 r_4 + r_2 r_3) + \gamma_Y r_1 r_2 \\ r_0(\beta_Y r_4 + \alpha_Y r_2) \\ -r_0(\alpha_Y r_4 + \gamma_Y r_2) \\ \beta_Y r_3^2 + 2\alpha_Y r_1 r_3 + \gamma_Y r_1^2 \\ -r_0(\beta_Y r_3 + \alpha_Y r_1) \quad r_0^2 \beta_Y \\ (\alpha_Y r_3 + \gamma_Y r_1) \quad -r_0^2 \alpha_y \quad r_0^2 \gamma_Y \end{pmatrix} \tag{24}$$

Comparing the beam envelope and measured envelope, extended Twiss parameters are obtained. Upper two lines in Eq. 23 are used for X mode, while lower two lines in Eq. 24 are used for Y mode. The correlations among y or p_y in X mode is contaminated by a leak of Y mode, vice versa.

Betatron phase advance between two monitors is given by taking the correlation of the two monitor position.

$$\cos(\phi_{X,i+1} - \phi_{X,i}) = \frac{\langle x(s_{i+1}) x(s_i) \rangle}{\sqrt{\langle x(s_{i+1})^2) \rangle \langle x(s_i)^2 \rangle}} \tag{25}$$

Figures 2 and 3 show measured beta function and x-y coupling parameters. Measurement of beta function is done by x(y) signal for X(Y) mode oscillation, while that of x-y coupling is done by y signal for X mode oscillation, vice versa. Reliability of the beta measurement is much better than coupling. Calibration of monitor for rotation is unavoidable. At present the reliability of x-y coupling measurement is not very good.

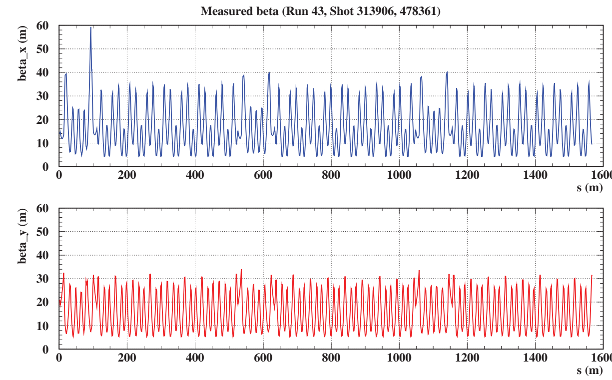

Figure 2: Measured beta function.

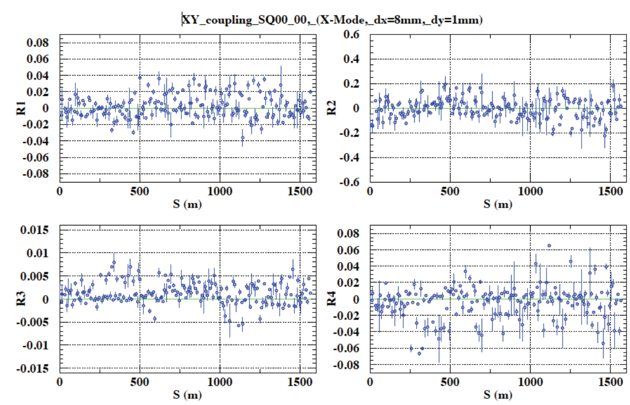

Figure 3: Measured xy coupling parameters.

LINEAR APPROXIMATION: BEAM ENVELOPE FORMALISM BASED ON MEASURED EXTENDED TWISS PARAMETERS

Beam envelope matrix is defined by averaging the beam particle position in the phase space,

$$\langle \boldsymbol{x}(s) \boldsymbol{x}^T(s) \rangle \tag{26}$$

where the center of mass is subtracted in $\boldsymbol{x}$.

Space charge force is linearized in the envelope formalism [5, 6]. The force with an beam envelope is expressed by a matrix transformation,

$$M_\Phi = T^{-1}(\theta) \begin{pmatrix} 1 & 0 & 0 & 0 \\ k_x & 1 & 0 & 0 \\ 0 & 0 & 1 & 0 \\ 0 & 0 & k_y & 1 \end{pmatrix} T(\theta) \tag{27}$$

where T is rotation matrix in the real coordinate space.

$$T(\theta) = \begin{pmatrix} \cos\theta & 0 & \sin\theta & 0 \\ 0 & \cos\theta & 0 & \sin\theta \\ -\sin\theta & 0 & \cos\theta & 0 \\ 0 & -\sin\theta & 0 & \cos\theta \end{pmatrix} \tag{28}$$

The angle θ is tilt of the ellipse of the beam envelope in the real coordinate space. The angle is expressed by the beam envelope as follows,

$$\tan 2\theta = \frac{\langle xy \rangle}{\langle x^2 \rangle - \langle y^2 \rangle} \tag{29}$$

The linearized force of the space charge k_i is determined by the beam size along the principle axis (a, b).

$$k_x = \frac{4r_p\lambda}{\beta^2\gamma^3} \frac{1}{a(a+b)} \qquad k_y = \frac{4r_p\lambda}{\beta^2\gamma^3} \frac{1}{b(a+b)}, \tag{30}$$

ISBN 978-3-95450-118-2

where r_p and λ are the proton classical radius and line density of the proton beam, respectively. The sizes are expressed by

$$a^2 = \langle x^2 \rangle \cos^2\theta + \langle xy \rangle \sin 2\theta + \langle y^2 \rangle \sin^2\theta \quad (31)$$

$$b^2 = \langle x^2 \rangle \sin^2\theta - \langle xy \rangle \sin 2\theta + \langle y^2 \rangle \cos^2\theta \quad (32)$$

The transfer matrix is expressed by product of the transfer matrices for zero intensity and for the space charge force as follows,

$$M(s', s) = \prod_{i=0}^{N'-1} M_0(s_{i+1}, s_i) M_\Phi(s_i) \quad (33)$$

The revolution matrix is given by the same way, $s' = s + C$.

The beam envelope is transferred by the matrices as follows

$$\langle \boldsymbol{x}(s')\boldsymbol{x}^T(s') \rangle = M(s', s) \langle \boldsymbol{x}(s)\boldsymbol{x}^T(s) \rangle M^T(s', s) \quad (34)$$

where $s_0 = s$, $s_{N'} = s'$.

The beam envelope is transferred by the revolution matrix. Equilibrium envelope in linear approximation is given by applying the periodic boundary condition to the envelope,

$$M(s) \langle \boldsymbol{x}\boldsymbol{x}^T \rangle M^T(s) = \langle \boldsymbol{x}\boldsymbol{x}^T \rangle \quad (35)$$

Since $M_\Phi(s_i)$ contains the beam envelope, the solution is given self-consistently. The solution is given by

$$\langle \boldsymbol{x}\boldsymbol{x}^T \rangle = V^{-1} \begin{pmatrix} \varepsilon_X & 0 & 0 & 0 \\ 0 & \varepsilon_X & 0 & 0 \\ 0 & 0 & \varepsilon_Y & 0 \\ 0 & 0 & 0 & \varepsilon_Y \end{pmatrix} (V^{-1})^t \quad (36)$$

Solving the periodic M, which means obtaining self-consistent extended Twiss parameters, is equivalent to solving equilibrium envelope.

Figure 4 shows self-consistent coupling parameters.

NONLINEAR SPACE CHARGE EFFECT WITH THE MEASURED EXTENDED TWISS PARAMETERS

Accelerators are designed so that nonlinear components are placed with a symmetry to avoid structure resonances. Symmetry of linear optics guarantees to suppress space charge origin resonances. For example, sextupoles and space charge force do not induce skew resonance component in the design lattice. Super-periodicity for the beta function suppresses resonances except for structured one. The symmetry of the design lattice is broken in actual accelerators. In general people generate random errors in accelerator components, and evaluate the effects of the errors. However such error lattice is mere a sample of random generation.

Now the design transfer matrix is replaced by the measured transfer matrix. One turn map including space charge

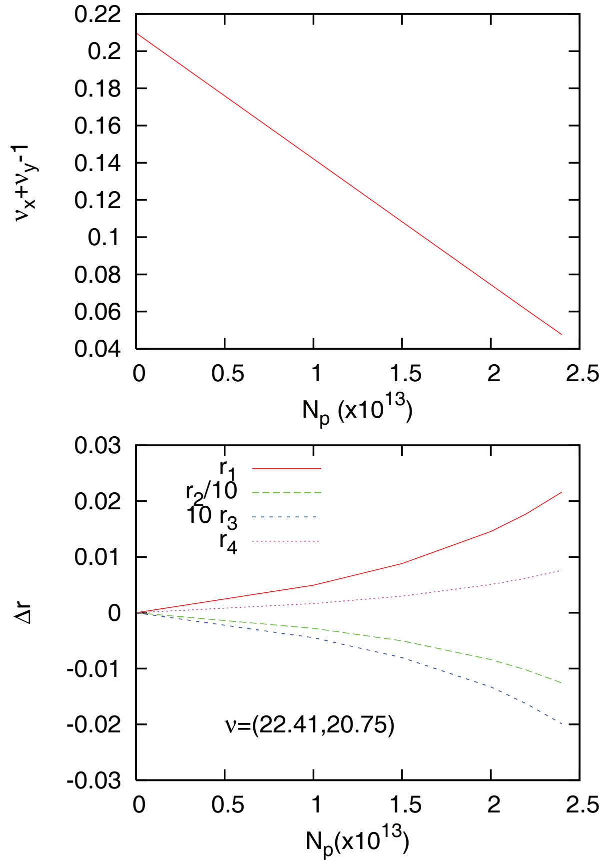

Figure 4: (Preliminary) Tune summation (top) and x-y coupling parameters (bottom) given by solving the beam envelope equation.

force (Eq. 2) is expressed by the nonlinear transformation and linear transfer matrix as follows,

$$\mathcal{M}(s) = \prod_{i=0}^{N-1} M(s_{i+1}, s_i) e^{-:H_I(s_i):}, \quad (37)$$

where $N = N_{nl} + N_{sc}$, and $H_I = \Phi$ or H_{nl}.

The designed transfer matrix is corrected by measured extended-Twiss parameters V and measured betatron phase ΔU_i to replace with the measured one,

$$\begin{aligned} M(s_{i+1}, s_i) &= V^{-1}(s_{i+1}) U_{i+1,i} \Delta U_i V(s_i) \quad (38) \\ &= V^{-1}(s_{i+1}) V_0(s_{i+1}) M_0(s_{i+1}, s_i) V_0^{-1}(s_i) \Delta U_i V(s_i) \end{aligned}$$

In the simulation, the operations $V^{-1}(s_{i+1})V_0(s_{i+1})$ and $V_0^{-1}(s_i)\Delta U_i V(s_i)$ are inserted in the transfer map between s_i to s_{i+1}.

We can evaluate effects of the optics errors at sextupole and space charge force one by one. Some preliminary results are presented in the last part of this paper. Figure 5 shows the beam loss for several cases. In top picture, optics errors $V = B_{mes}R_{mes}$ is used in space charge force, while $V = B_0R_0$ (red), $V = B_{mes}R_{mes}$ (green), $V = B_{mes}R_0$ (blue) and $V = B_0R_{mes}$ (magenta) are

ISBN 978-3-95450-118-2

used in sextupoles, respectively. In bottom picture, optics errors $V = B_0 R_0$ is used in sextupoles, while $V = B_0 R_0$ (red), $V = B_{mes} R_{mes}$ (green), $V = B_{mes} R_0$ (blue) and $V = B_0 R_{mes}$ (magenta) are used in sextupole, respectively. Betatron phase shift ΔU is not taken into account yet. The coupling errors in sextupole magnets degrade the

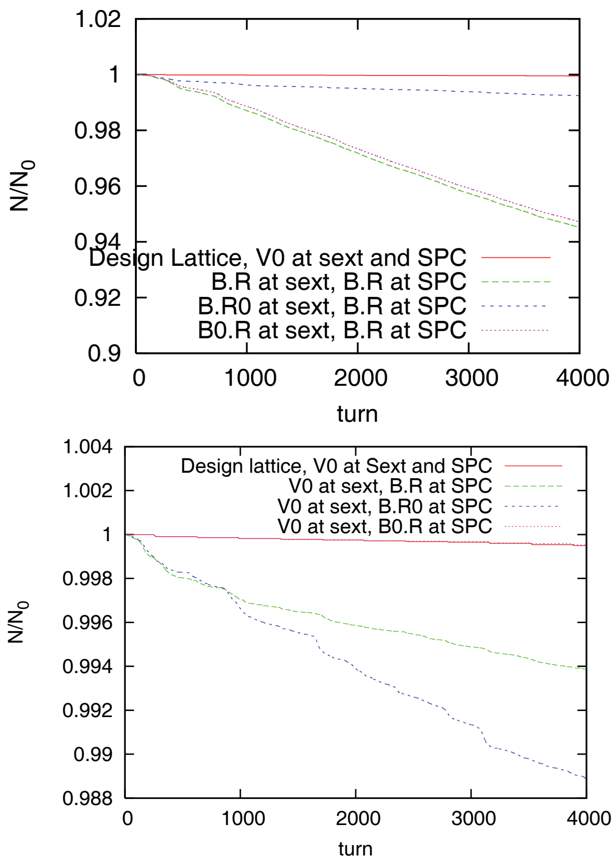

Figure 5: (Preliminary) Beam loss for various cases of V given by simulation.

beam loss dominantly.

Figure 6 shows the intensity dependence of the beam loss for two cases. In Top picture, $V = B_{mes} R_{mes}$ is used in space charge force and sextupoles. In bottom picture, $V = B_{mes} R_{mes}$ is used in space charge force, while $V = B_0 R_0$ in sextupoles.

SUMMARY

Transfer and revolution matrices are parametrized by the extended Twiss parameters and betatron phase. These quantities are measurable using turn-by-turn monitors at J-PARC MR. The measured transfer and revolution matrices are used in linear envelope equation and space charge simulations. x-y coupling at sextupoles seems dominant for the beam loss. Space charge force may be role of tune spread source.

In the next step, we should understand the mechanism, which resonances are induced. It should be clear consis-

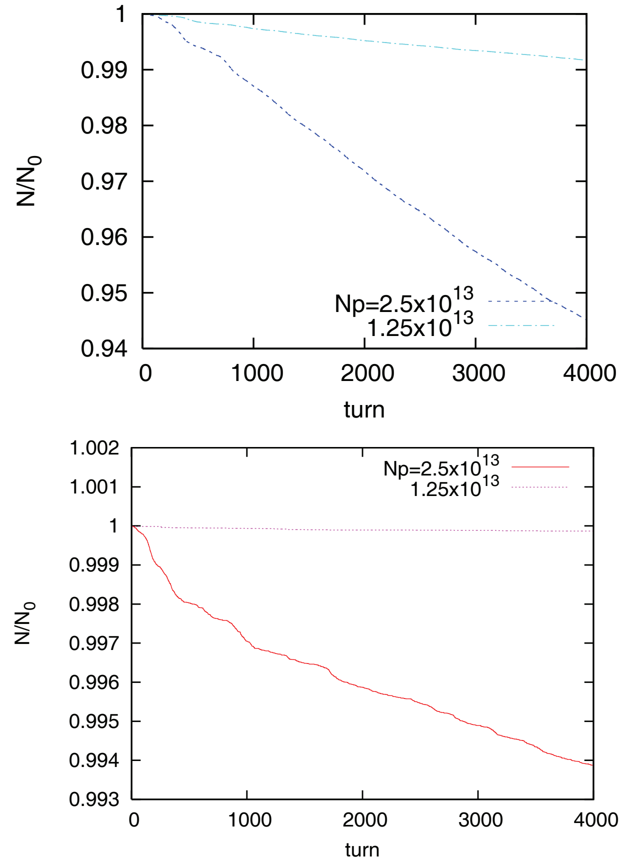

Figure 6: (Preliminary) Intensity dependence of the beam loss. Top picture is obtained for $V = B_{meas.} R_{meas.}$ at both of space charge and sextupoles. Bottom picture is obtained for $V = B_{meas.} R_{meas.}$ at space charge and $V = B_0 R_0$ at sextupoles.

tency with the beam envelope theory. Most important issue is to establish the reliability of x-y coupling measurement, and development of the correction scheme of the extended Twiss parameters.

REFERENCES

[1] K. Ohmi et al., Proceedings of HB2009.

[2] K. Ohmi, K. Hirata, K. Oide, Phys. Rev. E49, 751 (1994).

[3] Y. Seimiya et al., Progress of Theoretical Phyiscs, 127, 1099 (2012).

[4] Y. Ohnishi et al., Phys. Rev. ST-AB 12, 091002 (2009).

[5] D. Chernin, Particlr Accelerators, 24, 29 (1988).

[6] G.Franchetti, I. Hofmann, M. Aslaninejad, PRL 94, 194801 (2005).

ISBN 978-3-95450-118-2